Kruglyakov and Kuvshinov
*Earth, Planets and Space* (2019) 71:4
https://doi.org/10.1186/s40623-018-0972-8

Earth, Planets and Space

EXPRESS LETTER

Open Access

# 3-D inversion of MT impedances and inter-site tensors, individually and jointly. New lessons learnt

Mikhail Kruglyakov[1,2*†] and Alexey Kuvshinov[1†]

**Abstract**

A conventional magnetotelluric (MT) survey layout implies measurements of horizontal electric and magnetic fields at every site with subsequent estimation and interpretation of impedance tensors $Z$ or dependent responses, such as apparent resistivities and phases. In this work, we assess advantages and disadvantages of complementing or substituting conventional MT with inter-site transfer functions such as inter-site impedance tensor, $Q$, horizontal magnetic, $M$, and horizontal electric, $T$, tensors. Our analysis is based on a 3-D inversion of synthetic responses calculated for a 3-D model which consists of two buried adjacent (resistive and conductive) blocks and thin resistor above them.The (regularized) 3-D inversion is performed using scalable 3-D MT inverse solver with forward modelling engine based on a contracting integral equation approach. The inversion exploits gradient-type (quasi-Newton) optimization algorithm and invokes adjoint sources approach to compute misfits' gradients. From our model study, we conclude that: (1) 3-D inversion of either $Z$ or $Q$ tensors recovers the "true" structures equally well. This, in particular, raises the question whether we need magnetic field measurements at every survey site in the course of 3-D MT studies; (2) recovery of true structures is slightly worse if $T$ tensor is inverted, and significantly worse if $M$ tensor is inverted; (3) simultaneous inversion of $Z$ and $M$ (or $Z$ and $T$) does not improve the recovery of true structures compared to individual inversion of $Z$ or $Q$; (4) location of reference site, which is required for calculating inter-site $Q$, $T$ and $M$ tensors, has also marginal effect on the inversion results.

**Keywords:** Magnetotellurics, 3-D inversion, Inter-site tensors

## Introduction

One of the well-established geophysical techniques to explore the Earth's interiors is magnetotelluric (MT) method (Chave and Jones 2012). During an MT survey, natural variations of the horizontal electric, $\mathbf{E}_\tau$, and magnetic, $\mathbf{H}_\tau$, fields are measured with further translating them into subsurface's electrical conductivity distribution. Conductivity is ultimately interpreted in terms of Earth's composition, temperature, volatile content and partial melt. It is assumed in MT that the source of time-varying fields $\mathbf{E}_\tau$ and $\mathbf{H}_\tau$ is vertically incident plane wave of variable polarization. The plane wave assumption allows one to write an equation which relates frequency domain $\mathbf{E}_\tau$ and $\mathbf{H}_\tau$ at a survey site $\mathbf{r}_s$ via complex-valued impedance tensor $Z$ (Berdichevsky and Dmitriev 2008)

$$\mathbf{E}_\tau(\mathbf{r}_s,\omega) = Z(\mathbf{r}_s,\omega)\mathbf{H}_\tau(\mathbf{r}_s,\omega), \quad Z = \begin{pmatrix} Z_{xx} & Z_{xy} \\ Z_{yx} & Z_{yy} \end{pmatrix}, \qquad (1)$$

where $\omega$ is angular frequency, $\mathbf{E}_\tau = [E_x, E_y]^{\mathrm{T}}$, $\mathbf{H}_\tau = [H_x, H_y]^{\mathrm{T}}$, and the superscript (T) denotes the transpose of a vector. Estimation of $Z$ at multiple survey sites and frequencies, with subsequent inversion of the estimated $Z$ in terms of subsurface conductivity constitute an essence of MT method. Starting with 1-D MT inversions, and thereafter 2-D, nowadays 3-D MT inversions has become common practice due to the availability of efficient and scalable 3-D forward modelling solvers and high-performance clusters. However, a proper

*Correspondence: m.kruglyakov@gmail.com
†Mikhail Kruglyakov and Alexey Kuvshinov are contributed equally to this work.
[1] Institute of Geophysics, ETH Zurich, Sonneggstrasse 5, 8092 Zurich, Switzerland
Full list of author information is available at the end of the article

Springer Open

© The Author(s) 2019. This article is distributed under the terms of the Creative Commons Attribution 4.0 International License (http://creativecommons.org/licenses/by/4.0/), which permits unrestricted use, distribution, and reproduction in any medium, provided you give appropriate credit to the original author(s) and the source, provide a link to the Creative Commons license, and indicate if changes were made.

3-D inversion requires 2-D—preferably regular—grid of observations over the region of interest. Moreover, if one is interested in laterally detailed conductivity images the observation grid should be rather dense. This, in particular, means that MT survey would become logistically and instrumentally demanding, if conventional MT survey setup—which requires measurements of both electric and magnetic fields at each survey site—is invoked. It is relevant to notice that MT was originally introduced by Tikhonov (1950) and Cagniard (1953) in assumptions that the measurements are performed at a single site, and the conductivity distribution beneath this site is 1-D, which inevitably leads to necessity of measuring both fields at the site. In case of a non-1-D problem setup and multiple-site survey layout, the requirement to measure both fields at each site seems could be relaxed. One of the options, which is already in use (e.g., Comeau et al. 2018), is a measurement of both fields on a subset of survey sites (say, on a coarser grid) and measurement of electric field only on an entire (dense) grid. In this scenario, one needs to invert instead of single-site $Z$ the so-called inter-site impedances $Q$ (Hermance and Thayer 1975)

$$\mathbf{E}_\tau(\mathbf{r}_s,\omega) = Q(\mathbf{r}_s,\mathbf{r}_r,\omega)\mathbf{H}_\tau(\mathbf{r}_r,\omega), \quad Q = \begin{pmatrix} Q_{xx} & Q_{xy} \\ Q_{yx} & Q_{yy} \end{pmatrix}, \quad (2)$$

where $\mathbf{r}_r$ stands for the reference site(s) where both, electric and magnetic, fields are measured. Surprisingly enough no model study is reported yet with the discussion of advantages and disadvantages of complementing or substituting during 3-D MT inversion the conventional (single-site) impedances with inter-site impedances. In this paper, we fill this gap and compare results of 3-D inversion of $Z$ and $Q$. Our analysis is based on a 3-D inversion of synthetic responses calculated for a 3-D model which consists of two buried adjacent (resistive and conductive) blocks and thin resistor above them. We consider an ultimate case when both fields are available at one reference site and explore the dependence of the inversion results on the location of this site. For completeness, we also investigate the "performance" of a 3-D inversion if two alternative inter-site tensors, namely horizontal electric (telluric) tensor $T$ (Berdichevsky 1965; Yungul 1966)

$$\mathbf{E}_\tau(\mathbf{r}_s,\omega) = T(\mathbf{r}_s,\mathbf{r}_r,\omega)\mathbf{E}_\tau(\mathbf{r}_r,\omega), \quad T = \begin{pmatrix} T_{xx} & T_{xy} \\ T_{yx} & T_{yy} \end{pmatrix}, \quad (3)$$

and horizontal magnetic tensor $M$ (Berdichevsky and Dmitriev 2008)

$$\mathbf{H}_\tau(\mathbf{r}_s,\omega) = M(\mathbf{r}_s,\mathbf{r}_r,\omega)\mathbf{H}_\tau(\mathbf{r}_r,\omega), \quad M = \begin{pmatrix} M_{xx} & M_{xy} \\ M_{yx} & M_{yy} \end{pmatrix}, \quad (4)$$

are inverted. Here under "performance" we understand an ability of inversions to recover "true model"; note that the computational resources (memory, CPU time), needed to perform inversions of different tensors, are essentially the same. Final experiment we perform and discuss is a simultaneous inversion of $Z$ and $M$, and $Z$ and $T$.

We conclude the introduction with two remarks. The first refers to notations. We employ the notation $T$ for telluric tensor, following nomenclature which is routinely used in the literature where this type of responses is discussed (e.g., Berdichevsky 1965; Hermance and Thayer 1975; Yungul 1966). We know that many authors (e.g., Araya and Ritter 2016; Campanya et al. 2016) reserve $T$ for tippers—the single-site response functions that relate vertical and horizontal magnetic field components

$$H_z(\mathbf{r}_s,\omega) = W(\mathbf{r}_s,\omega)\mathbf{H}_\tau(\mathbf{r}_s,\omega), \quad W = [W_{zx} \quad W_{zy}]. \quad (5)$$

Here we use for tippers the notation $W$, following the original terminology [cf. Chapter 4 of Berdichevsky and Dmitriev (2008)]. The second remark concerns our decision not to discuss in the paper the 3-D inversion of $W$, and $Z$ and $W$. This is done by purpose, since we believe that this topic is already well covered in the literature (e.g Meqbel et al. 2014; Rao et al. 2014; Siripunvaraporn and Egbert 2009; Tietze and Ritter 2013; Yang et al. 2015).

## Modelling synthetic responses

To assess performance of 3-D inversion of different MT responses, we use the model from Grayver (2015). The model consists of three rectangular blocks embedded in homogeneous background half-space of conductivity 0.1 S/m ( cf. upper plots in Fig. 1). The shallow thin $3 \times 4 \times 0.3\,\mathrm{km}^3$ block of conductivity 0.002 S/m is located at the depth of 0.2 km and two deeper adjacent blocks of conductivities 1 S/m and 0.002 S/m, each of size $7 \times 4 \times 4.5\,\mathrm{km}^3$ are located at the depth of 1.5 km. Upper left and middle plots in Fig. 1 show plane view of the model at depths 300 and 2500 km, respectively. Upper right plot presents side view of the model taken along central, $y$-directed, profile, where $x$- and $y$-axes are pointed up and right, respectively, at "plane view" plots.

Synthetic responses (data) were generated at a regular 2-D $13 \times 13$ grid (black dots in upper left and middle plots of Fig. 1; spacing between grid points—1 km) for 16 frequencies evenly spaced on the logarithmic scale in the range of 0.001–100 Hz. Generation of the responses was performed using forward modelling code by Kruglyakov and Bloshanskaya (2017) which is based on contracting

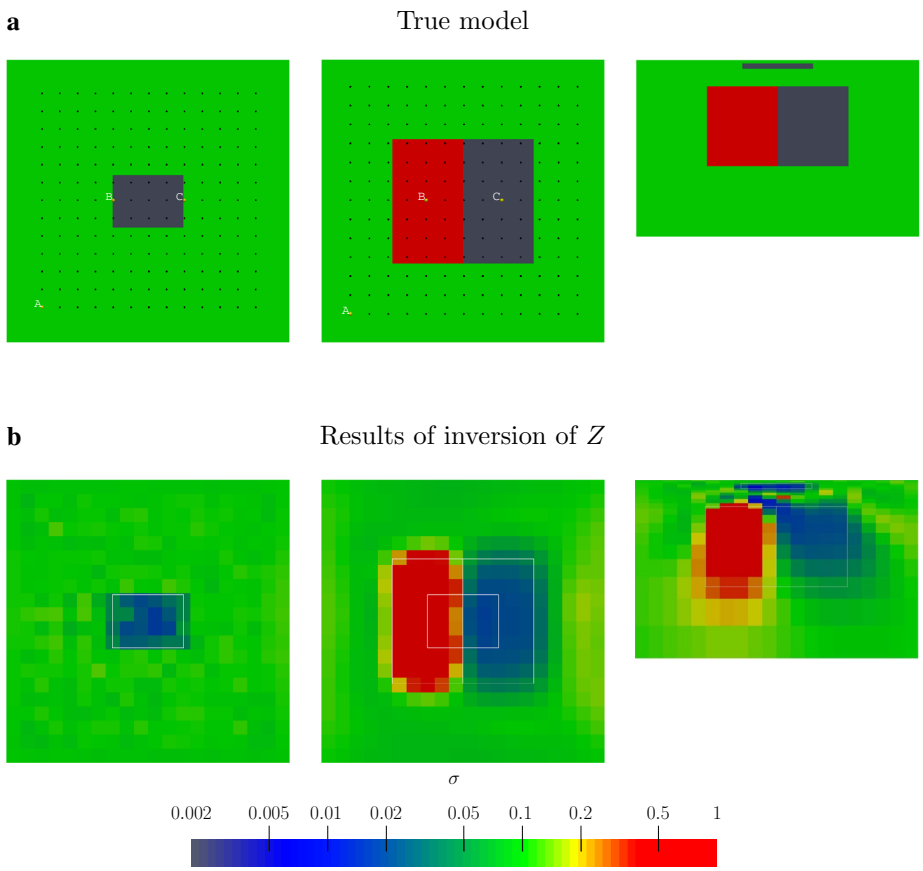


**Fig. 1** Upper left and middle plots show plane view of the model at depths 300 and 2500 m, respectively. Upper right plot presents the side view of the model. Side view is taken along central, *y*-directed, cross section, where *x*- and *y*-axes are pointed up and right, respectively, at "plane view" plots. Locations of survey sites are depicted by black dots in the plane view plots. Yellow dots in the same plots (denoted as A, B, C) stand for the locations of the reference site. Note that the reference site is only involved in the inversion of inter-site responses. Bottom plots show the model recovered by inversion of (single-site) impedances tensor $Z$. The results are shown through the same cross sections shown in upper plots. White lines depict the boundaries of the true model blocks

integral equation (CIE) approach (Pankratov et al. 1995; Singer 1995). Since CIE-based code was used for responses' generation, the forward modelling domain was confined to anomalous regions (three blocks) only. The blocks were discretized by cubic cells of equal size of $25 \times 25 \times 25\,\mathrm{m}^3$. Two percent random Gaussian noise was added to each element of the generated responses.

## Remarks on 3-D MT inverse solution

We exploit for (regularized) inversion our own, scalable, 3-D MT inverse solver which allows us to: (1) utilize different hardware from laptops to supercomputers; (2) deal with highly detailed and contrasting models, and (3) invert (separately or jointly) any type of single- or/and inter-site MT responses. Forward modelling code by Kruglyakov et al. (2016), also based on CIE approach, is called by inversion. To minimize target functional, the inverse solver uses gradient-type (quasi-Newton) optimization algorithm, namely BFGS (Nocedal and Wright 2006). This (conventional) functional consists of the corresponding misfit term and a stabilizer. Stabilizer is weighted with parameter $\lambda$ which regulates the smoothness of the model. In our implementation, a stabilizer approximates a gradient-like operator. The computation of misfit gradients is performed using adjoint sources formalism (Pankratov and Kuvshinov 2010).

During an inversion, one has to parametrize an inversion domain. We apply "mask parametrization" approach which allows us to merge any subset of forward modelling cells in order to account for (usually) irregular distribution of the observation sites and different resolution of MT data with respect to the depth. The sketch of such parametrization is demonstrated in Fig. 2.

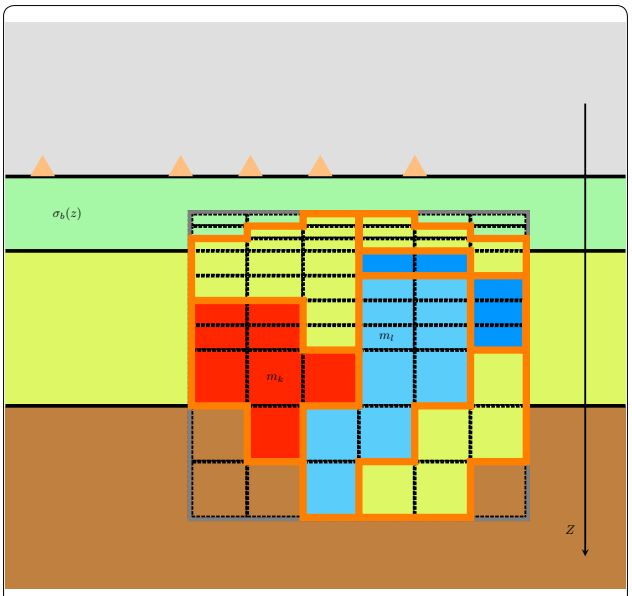


**Fig. 2** Sketch of mask parametrization. Grey line depicts the boundaries of the anomaly; black dotted lines denote the cells used in forward modelling; orange lines show the inversion domain cells

## Inversion setup

The inverse and forward modelling domains during inversion coincided and were set as $16 \times 16 \times 10\,\mathrm{km}^3$, thus including part of the volume occupied by the background medium. To diminish an "inverse crime," the forward modelling grid was taken different from that used for the responses' generation. Note that the inverse crime occurs when the same (or very nearly the same) ingredients are employed to synthesize as well as to invert data in an inverse problem; the first time the term is found in print seems to be in the book of Colton and Kress (1992). In lateral directions, the cell's size was set 4 times larger, i.e., $100 \times 100\,\mathrm{m}^2$, and in vertical direction the cell's size increased geometrically from 0.2 to 600 m with overall vertical discretization of $N_z = 120$. Thus forward modelling domain was discretized by $160 \times 160 \times 120$ cells. The inverse modelling domain was discretized by $20 \times 20 \times 40$ cells, i.e., one inverse modelling cell was a combination of $8 \times 8 \times 3$ forward modelling cells. 1-D section needed to calculate Green's tensors in the course of forward modelling was chosen to coincide with background 1-D section. Error floors of $0.02\sqrt{|e_{xx}|^2 + |e_{xy}|^2 + |e_{yx}|^2 + |e_{yy}|^2}$ were adopted, where $e_{xx}, \ldots, e_{yy}$ stand for elements of corresponding tensor at specific location. It is worth noting here that in case of $Z$ and $Q$ tensors the off-diagonal elements are dominant, whereas in case of $M$ and $T$ tensors—the diagonal elements are dominant.

## Results of inversion

### Inversion of (single-site) $Z$

Bottom plots in Fig. 1 demonstrates results of $Z$ inversion. Hereinafter the results of inversions are shown for the same cross sections as in upper plots of Fig. 1. Also, hereinafter the results are shown for the regularization parameter $\lambda$ which corresponds to the knee of the $L$-curve (Hansen 1992). One can observe from the figure that the shallow thin resistive block, as well as the buried conductive block, is recovered well, both in shapes and conductivity values. The recovery of buried resistive block is distinctly and expectedly worse; the image is blurred, and the block becomes less resolvable with depth.

Left upper plot in Fig. 3 shows cumulative (all periods, all sites, all tensor components) histograms of relative errors defined as

$$\frac{\left|e_{\alpha,\beta} - e^{\mathrm{mod}}_{\alpha,\beta}\right|}{\sqrt{|e_{xx}|^2 + |e_{xy}|^2 + |e_{yx}|^2 + |e_{yy}|^2}}, \tag{6}$$

where $\alpha, \beta = \{x, y\}$, $e_{\alpha,\beta}$ denote synthetic responses and $e^{\mathrm{mod}}_{\alpha,\beta}$—responses obtained either from starting or recovered models. The plot illustrates the fact that inversion gets to an appropriate target misfit given the number of data and noise in the data. Indeed, it is seen that substantially all normalized errors for the recovered model lie within target 2% error floor. Remarkably, the similar behaviour is observed for the histograms (cf. other plots in the figure) resulting from the inversions of inter-site responses to be discussed below.

### Inversion of inter-site tensors

The results of inversion of inter-site impedance tensor $Q$ are shown in Fig. 4. From top to bottom are the results for different location of the reference sites. These sites were placed, respectively, in an 1-D environment, above the centre of conductive and above the centre of deep resistive blocks. Their locations are depicted in upper left and middle plots of Fig. 1 by yellow dots A, B and C. It is seen from Fig. 4 that location of reference site has marginal effect on the inversion results. Remarkably, inversion of $Q$ recovers the "true" structures as good as inversion of $Z$ does (cf. bottom plots of Fig. 1).

Next we inverted horizontal electric tensor $T$. The results are shown in Fig. 5a for the case when the reference site was placed in an 1-D environment. We observe that results of inversion of $T$ are slightly worse than those obtained by inversion of either $Z$ or $Q$. The inversion results for the cases with (two) alternative locations of the

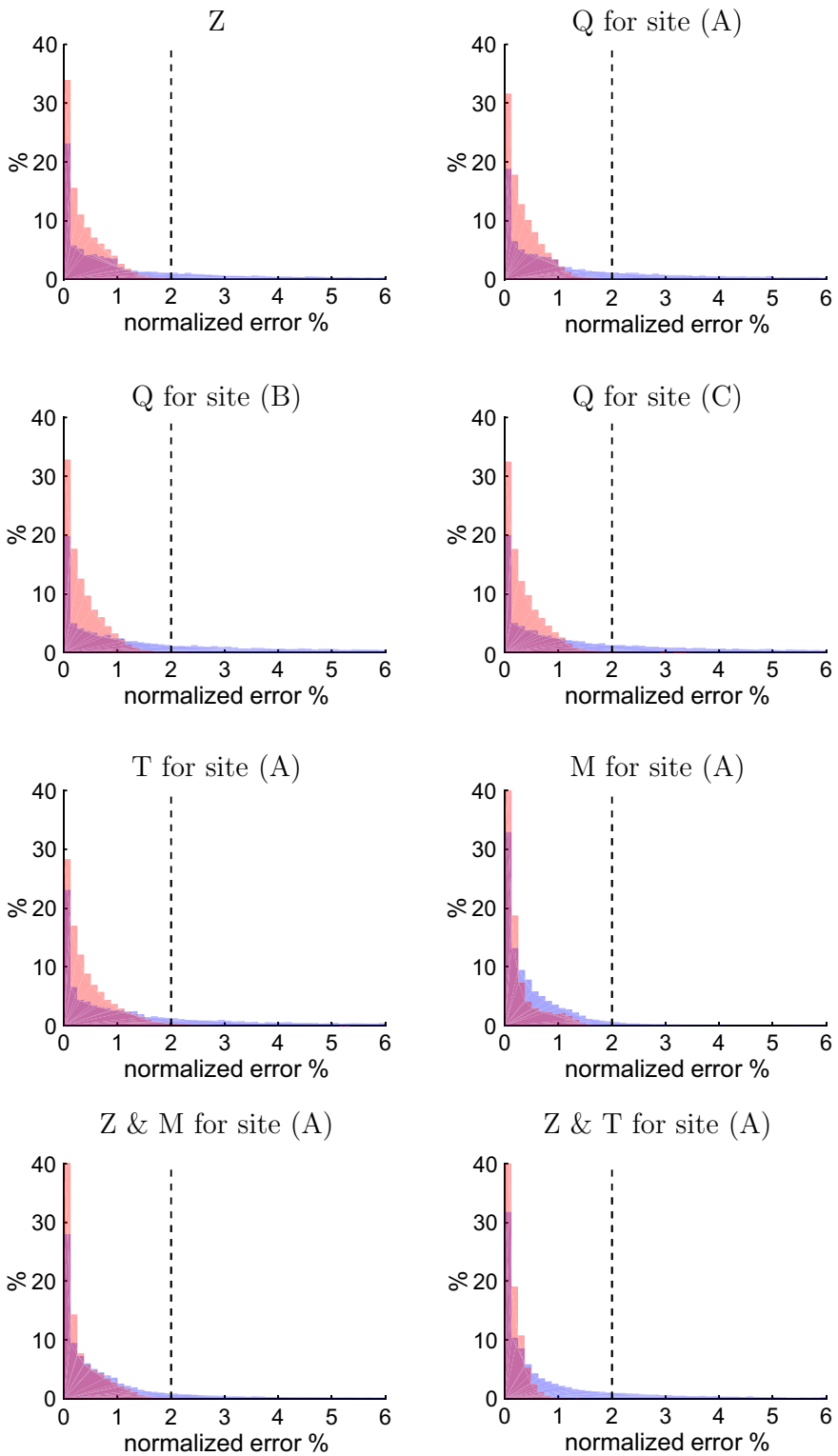


**Fig. 3** From left to the right and from top to bottom: cumulative (all periods, all sites, all components of corresponding tensors) histograms of absolute values of normalized errors for $Z$, $Q$, $T$, $M$, $Z$ and $M$, and $Z$ and $T$. Three plots for $Q$ show the results for three different locations of base site. Violet- and pink-coloured histograms stand for the cases when responses for starting and recovered models, respectively, were used for calculating errors. Vertical dashed line depicts target 2% error floor

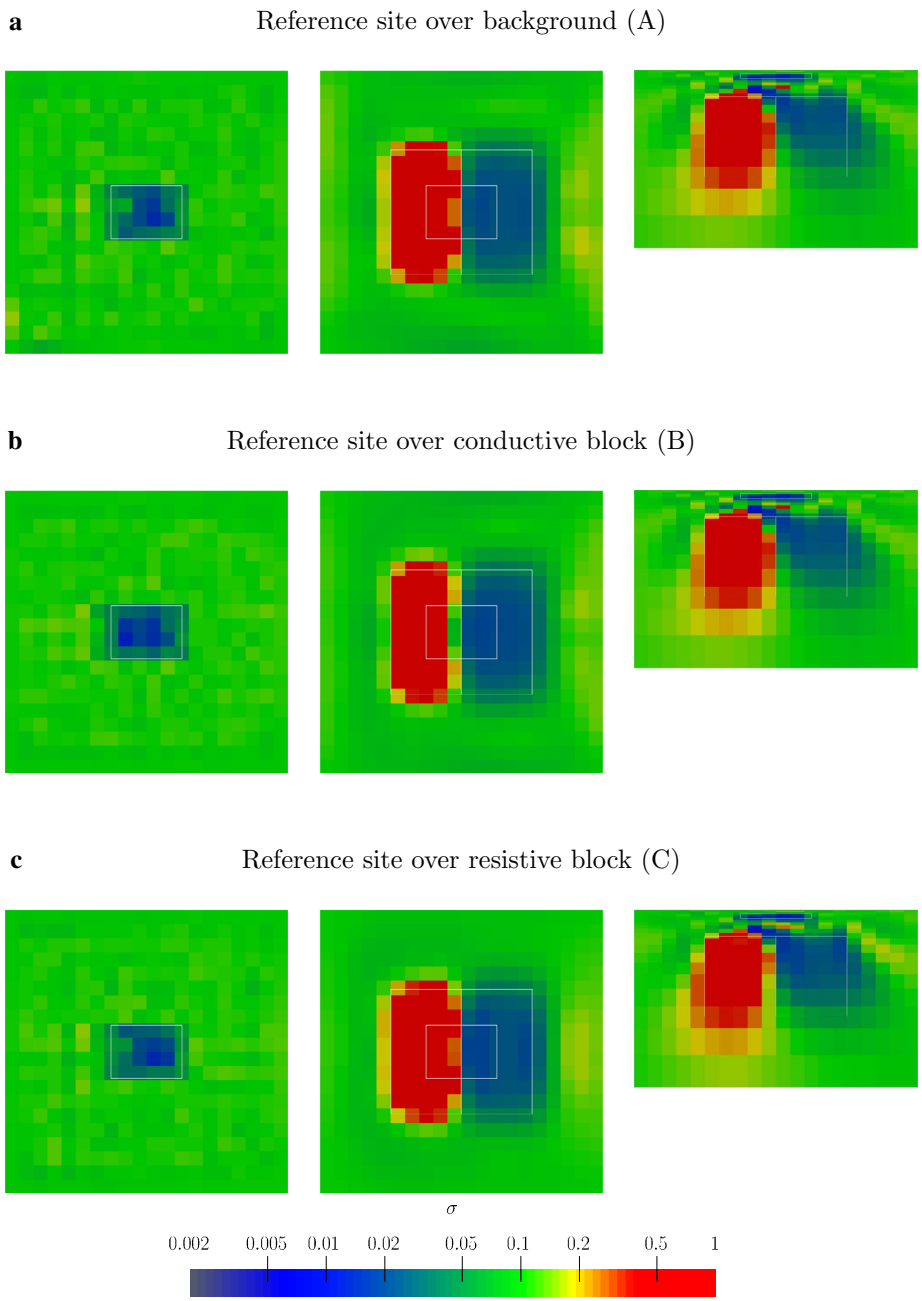


**Fig. 4** Model recovered by inversion of inter-site impedance tensor $Q$. The results are shown through the same cross sections as in upper plots of Fig. 1. From top to bottom are the results for different location of the reference site. Specifically, top, middle and bottom rows show the results for the cases when reference sites was placed in 1-D environment, above deep conductive, and deep resistive block, respectively

reference site are not shown since they—as in the case of inversion of inter-site impedances—differ insignificantly.

Further model experiment was the inversion of horizontal magnetic tensor $M$ (Fig. 5b) which was performed, again, for the case when the reference site was placed in an 1-D environment. The results of $M$ inversion turned out to be notably worse than those from inversion of $Z$, $Q$ or $T$, irrespective of reference site location (the results for $M$ inversion for other locations of reference site are not

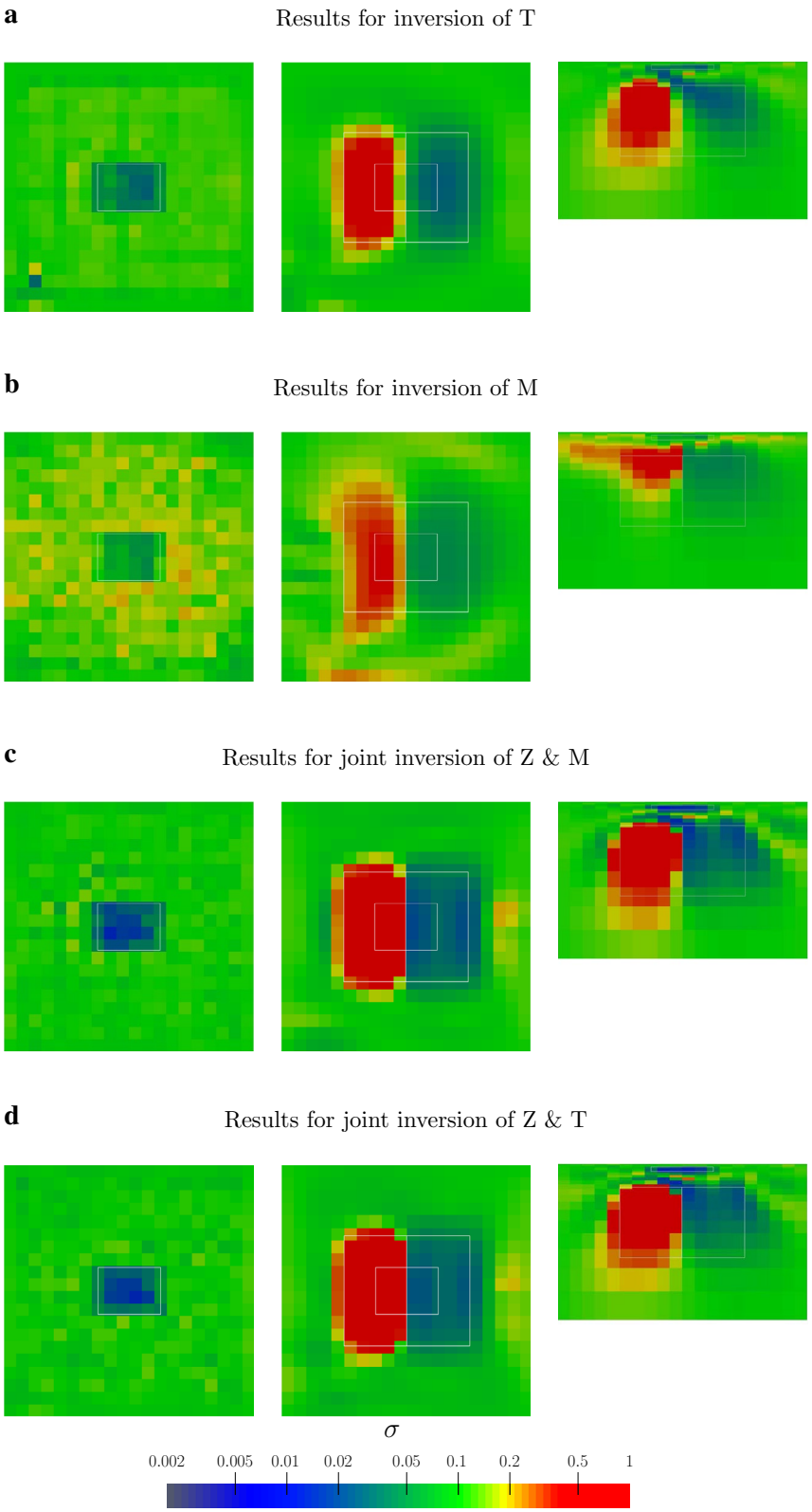


**Fig. 5** Models recovered by inversion of horizontal telluric tensor $T$ (**a**), horizontal magnetic tensor $M$ (**b**), by joint inversion of $Z$ and $M$ (**c**), and by joint inversion of $Z$ and $T$ (**d**). The results are shown through the same cross sections upper plots of Fig. 1, for the case when reference site was placed in 1-D environment

shown, since they were very similar, as it was in cases of $Q$, or $T$ inversions).

Final experiment we performed was simultaneous inversion of $Z$ and $M$, and $Z$ and $T$ (see Fig. 5c, d). Note that Campanya et al. (2016) also discussed inversion of $Z$ and $M$ (however using different 3-D model) and concluded that simultaneous inversion improves the recovery of true 3-D structures. Our inversion does not support this inference. Contrary, joint inversion of $Z$ and $M$ recovers true structures slightly worse than inversion of $Z$ (cf. bottom plots of Fig. 1). Simultaneous inversion of $Z$ and $T$ likewise does not reveal the improvement in the recovery of true structures compared with individual inversion of $Z$.

## Conclusions

We assessed in the paper the advantages and disadvantages of complementing or substituting conventional MT responses (impedances, $Z$) with inter-site transfer functions such as inter-site impedance tensor, $Q$, horizontal magnetic, $M$, and horizontal electric, $T$, tensors. Our analysis was based on a 3-D inversion of synthetic responses calculated for a 3-D conductivity model which included buried conductive and resistive blocks. From our model study, we conclude that 3-D inversion of either $Z$ or $Q$ recovers the "true" structure equally well. This, in particular, further promotes MT survey layout where measurements of both (electrical and magnetic) fields are conducted on a subset of survey sites (say, on a coarser grid, or even at a single reference site), and measurements of only electric field on an entire (dense) grid.

We also observed that recovery of the true structures is slightly worse if $T$ tensor is inverted, and considerably worse if $M$ tensor is inverted.

We attempted to improve the recovery of true 3-D structures by performing simultaneous inversion of $Z$ and $M$, or $Z$ and $T$; however, we found that such inversions did not do better job, compared to individual inversions of $Z$ or $Q$.

Finally, we note that the location of reference site, which is required for calculating inter-site $Q$, $T$ and $M$ tensors, had marginal effect on the inversion results.

#### Abbreviations

MT: magnetotelluric; BFGS: Broyden–Fletcher–Goldfarb–Shanno optimization algorithm.

#### Authors' contributions

AK initiated the study. MK performed forward and inverse modellings. MK and AK analysed and discussed the results, MK drafted the manuscript. Both authors read and approved the final manuscript.

#### Author details

[1] Institute of Geophysics, ETH Zurich, Sonneggstrasse 5, 8092 Zurich, Switzerland. [2] Geoelectromagnetic Research Center, The Schmidt Institute of Physics of the Earth, P.O.B. 30, Troitsk, Moscow, Russian Federation 108840.

#### Acknowlegements

The authors thank Colin Farquharson and Yosuo Ogawa for constructive comments on the manuscript. This work is partly supported by the Swiss National Science Foundation Grant No. ZK0Z2 163494, and the Swiss National Supercomputing Centre (CSCS) Grants (Projects IDs s660 and s828). The authors also acknowledge the team of HPC CMC Lomonosov MSU for access to Bluegene/P HPC.

#### Competing interests

The authors declare that they have no competing interests.

#### Availability of data and materials

Not applicable.

## Publisher's Note

Springer Nature remains neutral with regard to jurisdictional claims in published maps and institutional affiliations.

Received: 20 September 2018 Accepted: 8 December 2018
Published online: 14 January 2019

#### References

Araya J, Ritter O (2016) Source effects in mid-latitude geomagnetic transfer functions. Geophys J Int 204:606–630

Berdichevsky MN (1965) Electrical prospecting with the telluric current method. Q Colorado school of Mines 60(1). English translation of original 1960 Russian article

Berdichevsky MN, Dmitriev VI (2008) Models and methods of magnetotellurics. Springer, Berlin

Cagniard L (1953) Basic theory of the magnetotelluric method of geophysical prospecting. Geophysics 18:605–635

Campanya J, Ogaya X, Jones AG, Rath V, Vozar J, Meqbel N (2016) The advantages of complementing MT profiles in 3-D environments with geomagnetic transfer function and interstation horizontal magnetic transfer function data: results from a synthetic case study. GJI 207(3):1818–1836

Chave AD, Jones AG (2012) The magnetotelluric method—theory and practice. Cambridge University Press, Cambridge

Colton D, Kress R (1992) Inverse acoustic and electromagnetic scattering theory, applied mathematical sciences, vol 93. Springer, Berlin

Comeau M, Kaeufl J, Becken M, Kuvshinov A, Grayver A, Kamm J, Demberel S, Sukhbaatar U, Batmagnai E (2018) Evidence for fluid and melt generation in response to an asthenospheric upwelling beneath the Hangai Dome, Mongolia. Earth Planet Sci Lett 487:201–209

Grayver AV (2015) Parallel three-dimensional magnetotelluric inversion using adaptive finite-element method. Part I: theory and synthetic study. Geophys J Int 202(1):584. https://doi.org/10.1093/gji/ggv165

Hansen PC (1992) Analysis of discrete ill-posed problems by means of the L-curve. SIAM Rev 34:561–580

Hermance JF, Thayer RE (1975) Telluric-magnetotelluric method. Geophysics 40:664–668

Kruglyakov M, Bloshanskaya L (2017) High-performance parallel solver of electromagnetics integral equations based on Galerkin method. Math Geosci. https://doi.org/10.1007/s11004-017-9677-y

Kruglyakov M, Geraskin A, Kuvshinov A (2016) Novel accurate and scalable 3-D MT forward solver based on a contracting integral equation method. Comput Geosci 96:208–217. https://doi.org/10.1016/j.cageo.2016.08.017

Meqbel NM, Egbert GD, Wannamaker PE, Kelbert A, Schultz A (2014) Deep electrical resistivity structure of the northwestern U.S. derived from 3-D inversion of USArray magnetotelluric data. Earth Planet Sci Lett 402:290–304

Nocedal J, Wright SJ (2006) Numerical optimization. Springer, New York
Pankratov O, Kuvshinov A (2010) General formalism for the efficient calculation of derivatives of EM frequency-domain responses and derivatives of the misfit. Geophys J Int 181(1):229–249. https://doi.org/10.1111/j.1365-246X.2009.04470
Pankratov O, Avdeyev D, Kuvshinov A (1995) Electromagnetic-field scattering in a heterogeneous Earth: a solution to the forward problem. Izv Phys Solid Earth 31(3):201–209
Rao CK, Jones AG, Moorkamp M, Weckmann U (2014) Implications for the lithospheric geometry of the Iapetus suture beneath Ireland based on electrical resistivity models from deep-probing magnetotellurics. Geophys J Int 198:737–759
Singer B (1995) Method for solution of Maxwell's equations in non-uniform media. Geophys J Int 120:590–598
Siripunvaraporn W, Egbert G (2009) WSINV3DMT: vertical magnetic field transfer function inversion and parallel implementation. Phys Earth Planet Inter 173:317–329
Tietze K, Ritter O (2013) Three-dimensional magnetotelluric inversion in practice—the electrical conductivity structure of the San Andreas Fault in central California. Geophys J Int 195:130–147
Tikhonov AN (1950) On determining electrical characteristics of the deep layers of the Earth's crust. Doklady Akademii Nauk 73(2):295–297
Yang B, Egbert GD, Kelbert A, Meqbel N (2015) Three-dimensional electrical resistivity of the north-central USA from EarthScope long period magnetotelluric data. Earth Planet Sci Lett 422:87–93
Yungul S (1966) Telluric sounding—a magnetotelluric method without magnetic measurements. Geophysics 31(1):185

**Submit your manuscript to a SpringerOpen journal and benefit from:**

► Convenient online submission
► Rigorous peer review
► Open access: articles freely available online
► High visibility within the field
► Retaining the copyright to your article

**Submit your next manuscript at ► springeropen.com**